Electronic Supplementary Material (ESI) for Journal of Materials Chemistry A

Supporting Information

A microporous metal-organic framework assembled from am aromatic tetracarboxylate with the potential for hydrogen purification

Yabing He,[a] Shengchang Xiang,[b] Zhangjing Zhang,[b] Shunshun Xiong,[a] Chuande Wu,[c] Wei Zhou,[d,e] Taner Yildirim,[d,f] Rajamani Krishna,*[g] and Banglin Chen*[a]

[a] *Department of Chemistry, University of Texas at San Antonio, One UTSA Circle, San Antonio, Texas 78249-0698, United States; Fax: (1)-210-458-7428; E-mail: Banglin.Chen@utsa.edu; Homepage: www.utsa.edu/chem/chen.htlm*

[b] *Fujian Provincial Key Laboratory of Polymer Materials, Fujian Normal University, 3 Shangsan Road, Cangshang Region, Fuzhou 350007, China*

[c] *Department of Chemistry, Zhejiang University, Hangzhou 310027, China*

[d] *NIST Center for Neutron Research, Gaithersburg, Maryland 20899-6102, United States*

[e] *Department of Materials Science and Engineering, University of Maryland, College Park, Maryland 20742, United States*

[f] *Department of Materials Science and Engineering, University of Pennsylvania, Philadelphia, Pennsylvania 19104-6272, USA*

[g] *Van 't Hoff Institute for Molecular Sciences, University of Amsterdam, Science Park 904, 1098 XH Amsterdam, The Netherlands; E-mail: r.krishna@nva.nl*

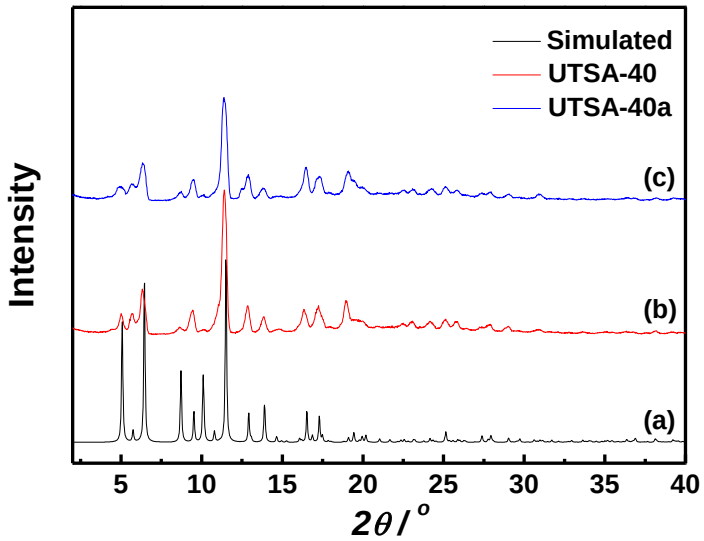

Figure S1. PXRD patterns of as-synthesized **UTSA-40** (b) and activated **UTSA-40a** (c) along with the simulated XRD pattern from the single-crystal X-ray structure (a).

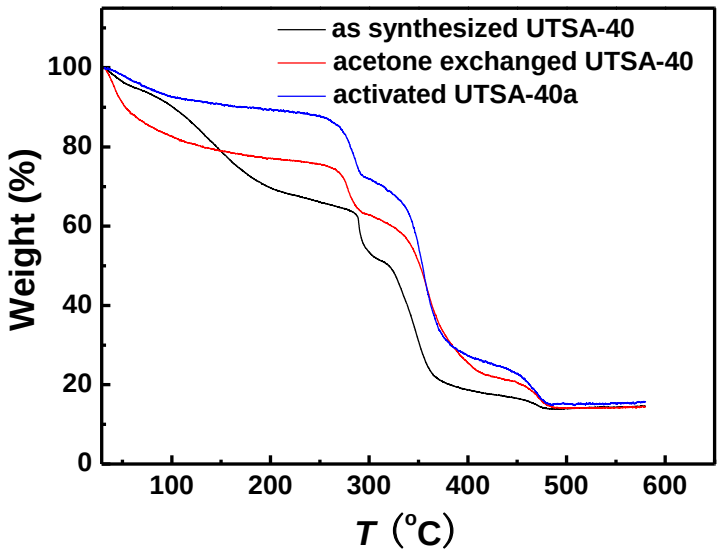

Figure S2. TGA curves of as-synthesized **UTSA-40** (black), acetone-exchanged **UTSA-40** (red), and activated **UTSA-40a** (blue) under a nitrogen atmosphere at a heating rate of 5 K min^{-1}.

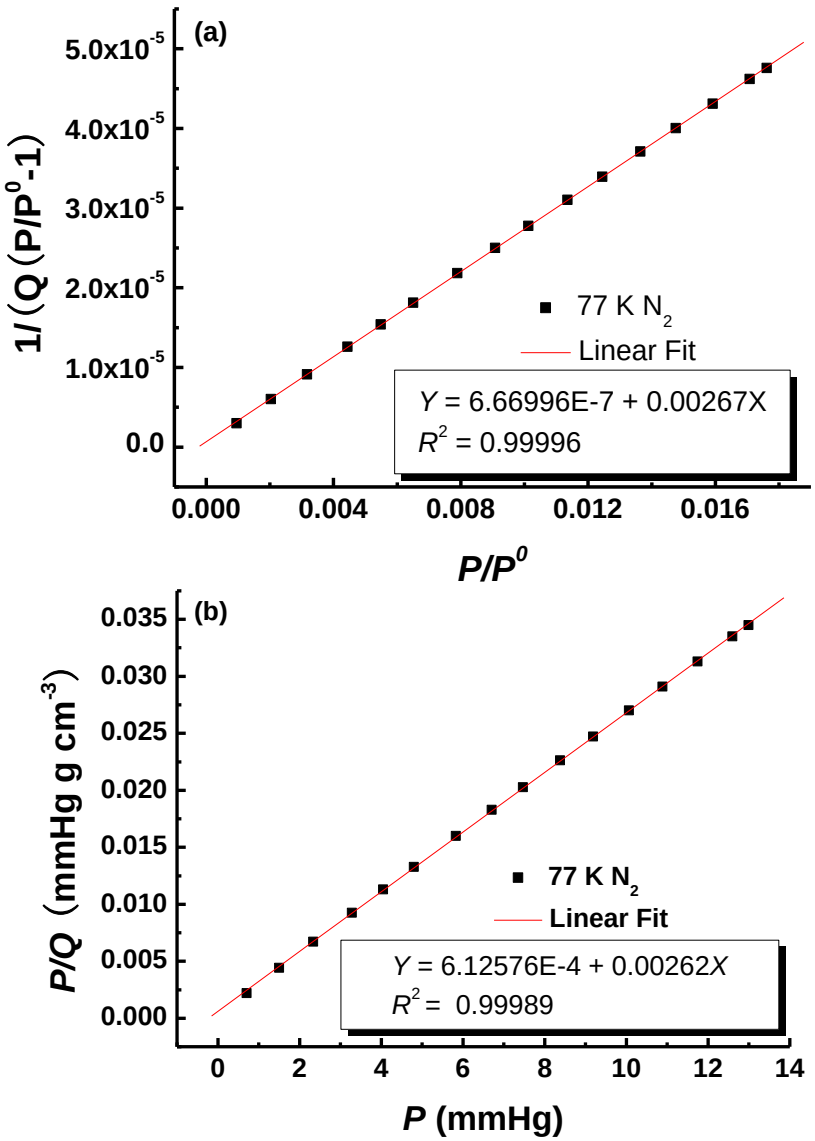

$$S_{BET} = (1/(6.66996 \times 10^{-7} + 0.00267))/22414 \times 6.023\times10^{23} \times 0.162 \times 10^{-18} = 1630.0\ m^2\ g^{-1}$$

$$\text{BET constant} = 1 + 0.00267/6.66996 \times 10^{-7} = 4004.0$$

$$S_{Langmuir} = (1/0.00262)/22414 \times 6.023 \times 10^{23} \times 0.162 \times 10^{-18} = 1661.5\ m^2\ g^{-1}$$

$$\text{Langmuir constant} = 0.00262/(6.12576 \times 10^{-4}) = 4.277\ mmHg^{-1} = 0.0321\ Pa^{-1}$$

Figure S3. BET (a) and Langmuir (b) plots of **UTSA-40a**.

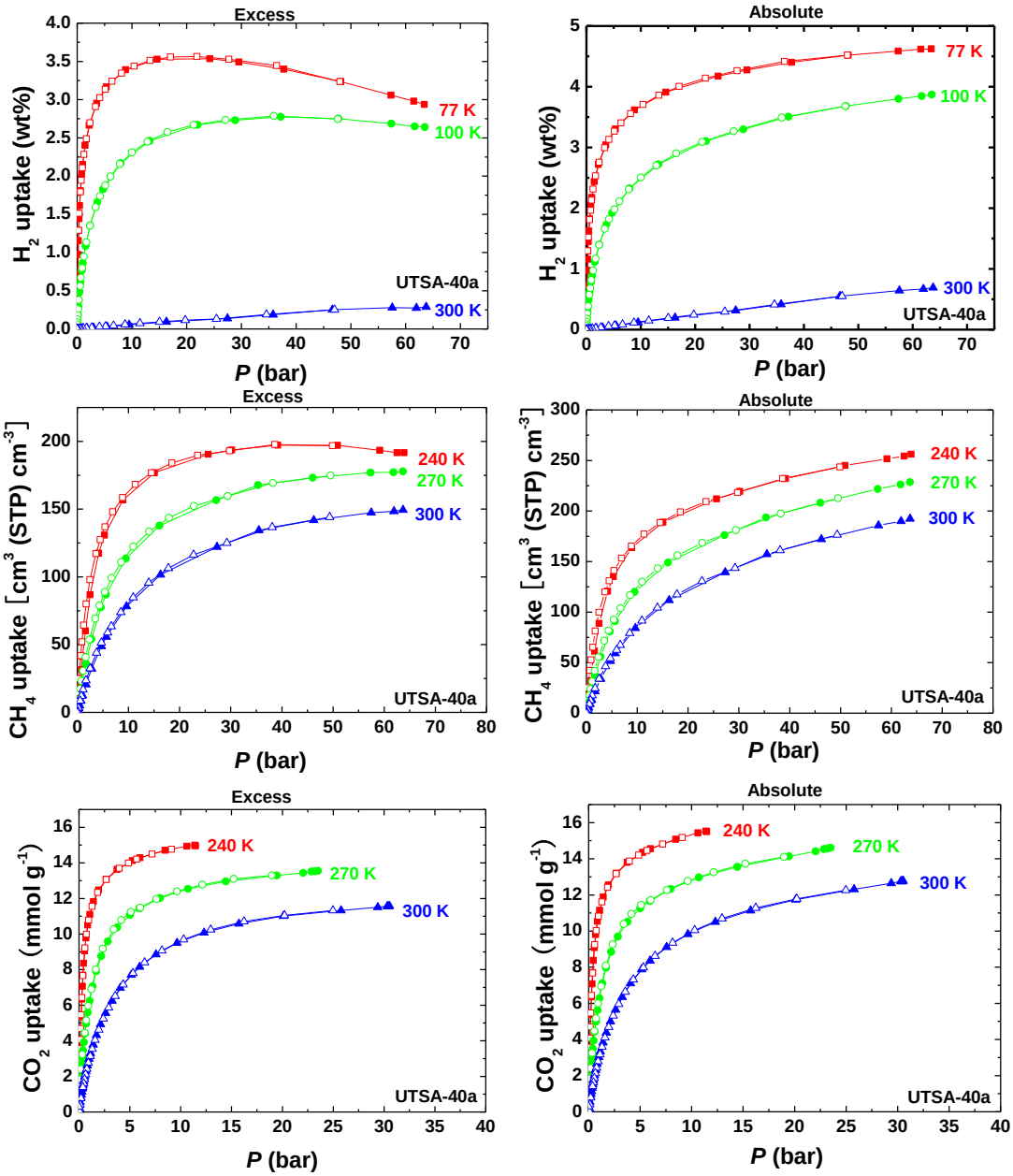

Figure S4. Excess and absolute high-pressure H_2, CH_4, and CO_2 sorption isotherms at three different temperatures. Solid symbols: adsorption; open symbols: desorption.

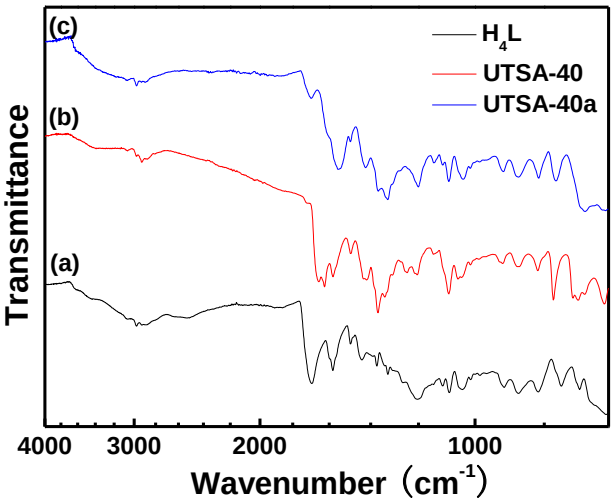

Figure S5. FTIR spectra of the organic linker H_4L (a), **UTSA-40** (b), and **UTSA-40a** (c).

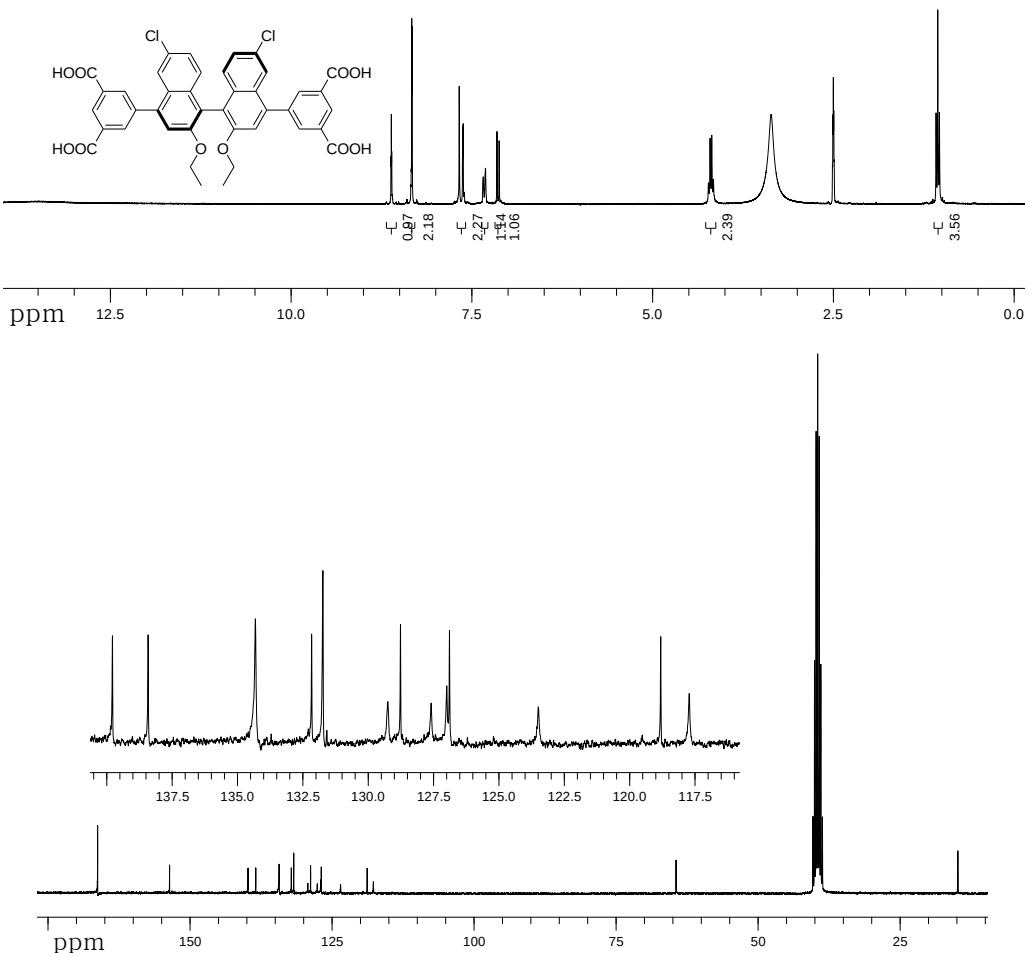

Figure S6. ^{1}H NMR (DMSO-d_6, 300.0 MHz) and ^{13}C NMR (DMSO-d_6, 75.4 MHz) spectra of the organic building block H_4L.

Table S1. Structural data on the different adsorbents evaluated in this study for comparison purposes. The data for **MgMOF-74** and **NaX** are from Herm et al.[1] and Krishna and Long[2]. The data for **MIL-101** are taken from Chowdhury et al.[3] The data for **Cu-TDPAT** are from Wu et al.[4] The data for **LTA-5A** are from Pakseresht et al.[5] and Sircar and Golden.[6]

MOFs	Surface area [m^2 g^{-1}]	Pore volume [cm^3 g^{-1}]	Framework density [kg m^{-3}]
UTSA-40a	1630	0.654	827
MgMOF-74	1800	0.573	905
Cu-TDPAT	1938	0.930	782
MIL-101	2674	1.380	440
NaX	950	0.280	1421
LTA-5A	450	0.250	1508

Table S2. Dual-site Langmuir fit parameters for adsorption of CO_2, and CH_4 in **UTSA-40a**. The fits for CO_2 are based on high-pressure isotherm data measured at 240 K, 270 K, and 300 K. The fits for CH_4 are based on two sets of isotherms: (a) low-pressure data measured at 273 K, and 296 K, and (b) high-pressure data measured at 240 K, 270 K, and 300 K. The fits are based on the entire data sets covering both pressure regions.

	Site A				Site B			
	$q_{A,sat}$ [mol kg^{-1}]	b_{A0} [$Pa^{-\nu_i}$]	E_A [kJ mol^{-1}]	ν_A	$q_{B,sat}$ [mol kg^{-1}]	b_{B0} $Pa^{-\nu_i}$	E_B [kJ mol^{-1}]	ν_B
CO_2	8.6	1.10×10^{-13}	27.6	1	7.4	4.12×10^{-10}	23.6	1
CH_4	14	1.13×10^{-9}	15	1				

Table S3. 1-site Langmuir fit parameters for pure H_2 isotherms in **UTSA-40a**. The fits are for a temperature of 298 K.

	$q_{A,sat}$ [mol kg^{-1}]	b_A [$Pa^{-\nu_i}$]	ν_A
H_2	19	3.4×10^{-8}	1

Table S4. Dual-Langmuir-Freundlich fit parameters for **MgMOF-74** (= Mg_2(dobdc) = **CPO-27-Mg**). These CO_2 fit parameters were determined by fitting adsorption isotherms for temperatures ranging from 278 K to 473 K; the fit parameters are those reported earlier in the work of Mason et al.[7] The CH_4 parameters were determined by fitting adsorption isotherm data reported in the works of and He et al.[8], Dietzel et al.[9] and Bao et al.[10] The H_2 parameters are obtained from absolute uptake data in **MgMOF-74** at 298 K reported by Yaghi,[11] a document that is available on the web. The uptake data is at 298 K, and therefore the fit parameters are valid only for 298 K.

	Site A				Site B			
	$q_{A,sat}$ [mol kg^{-1}]	b_{A0} [$Pa^{-\nu_i}$]	E_A [kJ mol^{-1}]	ν_A	$q_{B,sat}$ [mol kg^{-1}]	b_{B0} [$Pa^{-\nu_i}$]	E_B [kJ mol^{-1}]	ν_B
CO_2	6.8	2.44×10^{-11}	42	1	9.9	1.39×10^{-10}	24	1
CH_4	11	7.48×10^{-10}	18.2	1	5	1.64×10^{-11}	18.2	1
H_2	36	2.1×10^{-8}		1				

Table S5. Dual-Langmuir-Freundlich parameter fits for **Cu-TDPAT**. The parameters are those reported in the work of Wu et al.[4] Note that for CH_4 and H_2, the data is available only at 298 K. There was an unfortunate typographical error in the CO parameters reported in Table 3 of Supporting Information accompanying the paper by Wu et al;[4] we have therefore also included the correct parameters for CO (not considered in this work) in the Table below. The breakthrough and IAST calculations reported by Wu et al.[4] were performed with the correct parameter sets.

	Site A				Site B			
	$q_{A,sat}$ [mol kg^{-1}]	b_{A0} [Pa$^{-\nu_i}$]	E_A [kJ mol^{-1}]	ν_A	$q_{B,sat}$ [mol kg^{-1}]	b_{B0} [Pa$^{-\nu_i}$]	E_B [kJ mol^{-1}]	ν_B
CO_2	0.46	1.33×10^{-16}	72	1.2	23.9	2.91×10^{-9}	23.8	0.75
CO	23	2.47×10^{-8}	13.2	0.8	2	6.75×10^{-15}	17.7	1.8
CH_4	16	5.77×10^{-7}		1				
H_2	38.5	2.6×10^{-8}		1				

Table S6. Dual-site Langmuir fit parameters for pure component isotherms in **MIL-101**. The fits for CO_2, and CH_4 and H_2 are based on the experimental data of Chowdhury et al.[3] The fits for pure H_2 isotherms in **MIL-101** are based on the experimental data of Latroche et al.,[12] available only at 298 K. There was an unfortunate typographical error in the H_2 parameters reported in Table 12 of Supporting Information accompanying the paper by Wu et al.[4] The breakthrough and IAST calculations reported by Wu et al.[4] were performed with the correct parameter sets as given below.

	Site A				Site B			
	$q_{A,sat}$ [mol kg^{-1}]	b_{A0} [Pa$^{-\nu_i}$]	E_A [kJ mol^{-1}]	ν_A	$q_{B,sat}$ [mol kg^{-1}]	b_{B0} [Pa$^{-\nu_i}$]	E_B [kJ mol^{-1}]	ν_B
CO_2	47	2.22×10^{-10}	17.5	1	1.1	2.95×10^{-11}	36	1
CH_4	34	1.79×10^{-9}	9.9	1				
H_2	60	1.41×10^{-8}		1				

Table S7. Dual-site Langmuir fit parameters for adsorption of CO_2, CH_4 and H_2 in **NaX** zeolite. These parameters were determined by fitting adsorption isotherm data reported in the works of Belmabkhout et al.[13] and Cavenati et al.,[14] after converting the excess data to absolute loadings.

	Site A				Site B			
	$q_{A,sat}$ [mol kg^{-1}]	b_{A0} [Pa$^{-\nu_i}$]	E_A [kJ mol^{-1}]	ν_A	$q_{B,sat}$ [mol kg^{-1}]	b_{B0} [Pa$^{-\nu_i}$]	E_B [kJ mol^{-1}]	ν_B
CO_2	3.5	3.64×10^{-13}	35	1	5.2	6.04×10^{-11}	35	1
CH_4	4	3.66×10^{-10}	14	1	5	3.75×10^{-9}	14	1
H_2	18	2.43×10^{-9}	6	1				

Table S8. 2-site Langmuir-Freundlich fit parameters for pure CO_2, CH_4 and H_2 isotherms in **LTA-5A** zeolite. The fits for pure CO_2, CH_4 are derived from re-fitting the experimental data at 303 K presented in Table 1 of Pakseresht et al..[5] The isotherm fit for H_2 is based on the data presented in Figure 6 of Sircar and Golden,[6] which was combined with Configurational-Bias Monte Carlo simulation data.

	$q_{A,sat}$ [mol kg^{-1}]	b_A [Pa$^{-\nu_i}$]	ν_A	$q_{B,sat}$ [mol kg^{-1}]	b_B [Pa$^{-\nu_i}$]	ν_B
CO_2	1.84	1.89×10^{-4}	1.24	2.1	8.51×10^{-4}	0.64
CH_4	2	5.77×10^{-6}	1			
H_2	15	2.05×10^{-8}	1			

Table S9. Crystal data and structure refinement for **UTSA-40**.

Empirical formula	$C_{58}H_{74}Cl_2Cu_2N_6O_{20}$
Formula weight	1373.23
Temperature (K)	293(2)
Wavelength (Å)	1.54178
Crystal system, space group	Trigonal, $R3_2$
Unit cell dimensions	a = 18.5676(7) Å b = 18.5676(7) Å c = 52.205(3) Å α = 90° β = 90° γ = 120°
Volume (Å^3)	15586.8(12)
Z, Calculated density (g cm^{-3})	9, 1.3165
Absorption coefficient (mm^{-1})	1.750
F(000)	3762
Crystal size (mm)	0.41 × 0.23 × 0.15
θ range for data collection (°)	4.36 to 67.51
Limiting indices	$-17 \leq h \leq 22$, $-17 \leq k \leq 19$, $-54 \leq l \leq 61$
Reflections collected / unique	10908 / 5973 (R_{int} = 0.0386)
Completeness to θ = 67.51°	98.2 %
Absorption correction	Analytical
Max. and min. transmission	0.7786 and 0.5329
Refinement method	Full-matrix least-squares on F^2
Data / restraints / parameters	5973 / 72 / 186
Goodness-of-fit on F^2	0.975
Final R indices [$I > 2\sigma(I)$]	R_1 = 0.0715, wR_2 = 0.1895
R indices (all data)	R_1 = 0.0962, wR_2 = 0.2237
Absolute structure parameter	0.12(10)
Largest diff. peak and hole (e Å^{-3})	0.548 and -0.272
CCDC	896825

Table S10. Gas sorption in the reported copper-tetracarboxylate frameworks.

Ligands MOFs	BET (Langmuir) [m^2 g^{-1}]	V_p [cm^3 g^{-1}]	D_c [g cm^{-3}]	H_2	CH_4 [cm^3 cm^{-3}]	CO_2 [mmol g^{-1}]	Ref
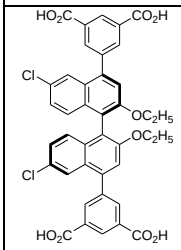 **UTSA-40**	1630 (1661)	0.65	0.827	2.2%, 18.2 g/L (77 K/1 bar)[a] 4.6%, 38.1 g/L (77 K/60 bar)[b] 0.7%, 5.8 g/L (300 K/60 bar)[b]	156[b](134[a]) (300 K/35 bar) 188[b](149[a]) (300 K/60 bar)	12.7 (300 K/30 bar)[b]	This work
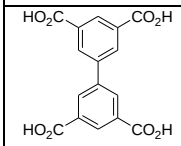 **MOF-505** **NOTT-100**	1670	0.68	0.927	2.59%, 24.0 g/L (77 K/1 bar)[b] 4.02%, 37.3 g/L (77 K/20 bar)[b]			15, 16
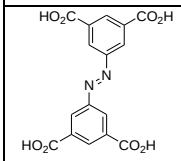 **PCN-10** **JUC-62**	2850	1.00	0.77	2.87%, 22.0 g/L (77 K/1 atm)[a] 6.76%, 51.9 g/L (77 K/50 bar)[b] Q = 11.60 kJ mol^{-1}			17, 18, 19
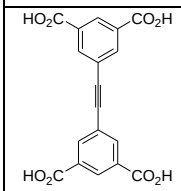 **PCN-16**	2273 (2800)	1.06	0.72	2.6%, 18.8 g/L (77 K/1 atm)[a] 4.9 wt%, 35.5 g/L (77 K/20 bar)[a]	175 (300 K/45 bar)[a]		20
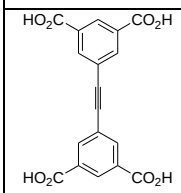 **PCN-16'**	1760 (2200)	0.84	0.76	1.7%, 13.0 g/L (77 K/1 atm)[a] 2.9 wt%, 22.2 g/L (77 K/20 bar)[a]	97 (300 K/45 bar)[a]		20
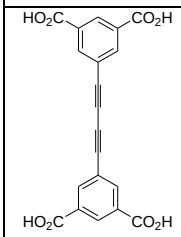 **PCN-46**	2500 (2800)	1.012	0.62	1.95%, 12.1 g/L (77 K/1 atm)[a] 6.88%, 45.7 g/L (77 K/97 bar)[b] Q = 7.2 kJ mol^{-1}	172 (298 K/35 bar)[b]	22.5 (298 K/ 30bar)[b]	21

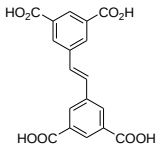 **PCN-11**	1931 (2442)	0.91	0.749	2.55%, 19.1 g/L (77 K/1 atm)[a] 5.05%, 37.8 g/L (77 K/20 bar)[a] 5.97%, 44.7 g/L (77 K/45 bar)[b] Q = 7 kJ mol^{-1}	171 (298 K/35 bar)[a] Q = 14.6 kJ mol^{-1}		18
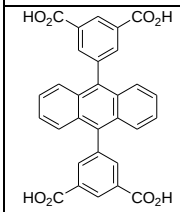 **PCN-14**	1753 (2176)	0.87	0.871		230[b] (290 K/35 bar)		22
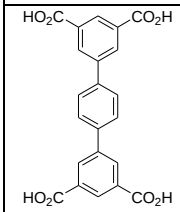 **NOTT-101**	2247	0.886	0.650	2.52%, 16.4 g/L (77 K/1 bar)[b] 6.06%, 39.4 g/L (77 K/20 bar) 6.60%, 43.1 g/L (77 K/60 bar)[b]			16
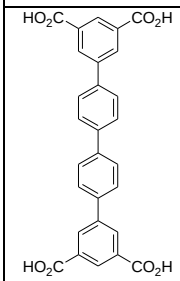 **NOTT-102**	2932	1.138	0.587	2.24%, 13.1 g/L (77 K/1 atm)[b] 6.07%, 35.6 g/L (77 K/20 bar)[b] 7.20%, 42.3 g/L (77 K/60 bar)[b] Q = 5.70 kJ mol^{-1}			16
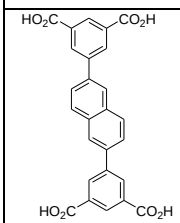 **NOTT-103**	2929	1.142	0.643	2.63%, 16.9 g/L (77 K/1 bar)[b] 6.51%, 41.9 g/L (77 K/20 bar)[b] 7.78%, 50.0 g/L (77 K/60 bar)[c]			23
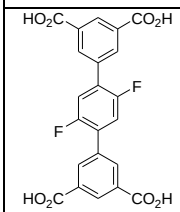 **NOTT-105**	2386	0.898	0.730	2.52%, 18.4 g/L (77 K/1 bar)[b] 5.40%, 39.4 g/L (77 K/20 bar)[b]			23

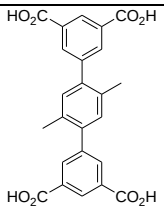 **NOTT-106**	1855	0.798	0.720	2.29%, 16.5 g/L (77 K/1 atm)[b] 4.50%, 32.4 g/L (77 K/20 bar)[b]			23
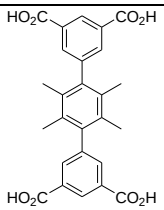 **NOTT-107**	1822	0.767	0.76	2.26%, 17.2 g/L (77 K/1 atm)[b] 4.46%, 33.8 g/L (77 K/20 bar)[b]			23
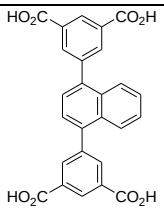 **NOTT-109**	1718	0.705	0.79	2.33%, 18.4 g/L (77 K/1 bar)[b] 4.15%, 32.8 g/L (77 K/20 bar)[b]			23
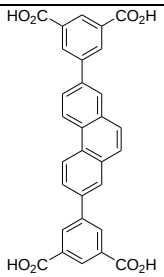 **NOTT-110**	2960	1.22	0.61	2.64%, 16.1 g/L (77 K/1 atm)[b] 6.59%, 40.5 g/L (77 K/20 bar)[b] 7.62%, 46.8 g/L (77 K/55 bar)[b] Q = 5.68 kJ mol^{-1}			24
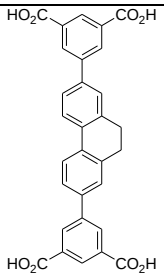 **NOTT-111**	2930	1.19	0.62	2.56%, 15.9 g/L (77 K/1 atm)[b] 6.48%, 40.0 g/L (77 K/20 bar)[b] 7.36%, 45.4 g/L (77 K/48 bar)[b] Q = 6.21 kJ mol^{-1}			24
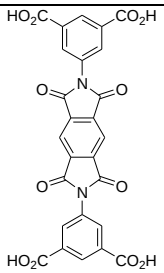 **SNU-50**	2300 (2450)	1.08	0.65	2.10%, 13.6 g/L (77 K/1 atm)[a] 7.85%, 51.0 g/L (77 K/60 bar)[b] 0.97%, 6.3 g/L (298 K/60 bar)[b] Q = 7.1 kJ mol^{-1}	155 (298 K/60 bar)[b] Q = 26.8 kJ mol^{-1}	17.5 (298 K/55 bar)[b]	25

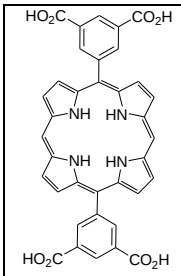 **MMPF-1**				Selective adsorption of H_2 and O_2 over N_2 at 77 K, and CO_2 over CH_4 at 196 K	26
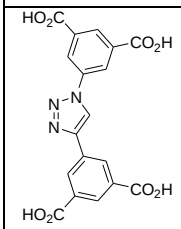 **NTU-101-Cu**	2017			1.78% H_2 at 77 K and 1 atm; 101 cm^3/g CO_2 at 273 K/1 atm; Selective adsorption of CO_2 over N_2 and CH_4	27
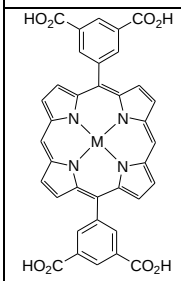	BET (Langmuir) surface areas: 647(864) m^2/g for M = Ni BET (Langmuir) surface areas: 498(613) m^2/g for M = Zn BET (Langmuir) surface areas: 379(486) m^2/g for M = Pd BET (Langmuir) surface areas: 509(680) m^2/g for M = $Mn(NO_3)$ BET (Langmuir) surface areas: 810(968) m^2/g for M = Ru(CO)				28

[a] excess adsorption; [b] absolute adsorption

Reference:

(1) Herm, Z. R.; Swisher, J. A.; Smit, B.; Krishna, R.; Long, J. R. Metal-Organic Frameworks as Adsorbents for Hydrogen Purification and Pre-Combustion Carbon Dioxide Capture *J. Am. Chem. Soc.* **2011**, *133*, 5664-5667.

(2) Krishna, R.; Long, J. R. Screening metal-organic frameworks by analysis of transient breakthrough of gas mixtures in a fixed bed adsorber, *J. Phys. Chem. C* **2011**, *115*, 12941-12950.

(3) Chowdhury, P.; Mekala, S.; Dreisbach, F.; Gumma, S. Adsorption of CO, CO_2 and CH_4 on Cu-BTC and MIL-101 Metal Organic Frameworks: Effect of Open Metal Sites and Adsorbate Polarity, *Microporous Mesoporous Mater.* **2012**, *152*, 246-252.

(4) Wu, H.; Yao, K.; Zhu, Y.; Li, B.; Shi, Z.; Krishna, R.; Li, J. Cu-TDPAT, an *rht*-type Dual-Functional Metal–Organic Framework Offering Significant Potential for Use in H_2 and Natural Gas Purification Processes Operating at High Pressures, *J. Phys. Chem. C* **2012**, *116*, 16609-16618.

(5) Pakseresht, S.; Kazemeini, M.; Akbarnejad, M. M. Equilibrium isotherms for CO, CO_2, CH_4 and C_2H_4 on the 5A molecular sieve by a simple volumetric apparatus, *Sep. Purif. Technol.* **2002**, *28*, 53-60.

(6) Sircar, S.; Golden, T. C. Purification of Hydrogen by Pressure Swing Adsorption, *Sep. Sci. and Technol.* **2000**, *35*, 667-687.

(7) Mason, J. A.; Sumida, K.; Herm, Z. R.; Krishna, R.; Long, J. R. Evaluating Metal-Organic Frameworks for Post-Combustion Carbon Dioxide Capture via Temperature Swing Adsorption, *Energy Environ. Sci.* **2011**, *3*, 3030-3040.

(8) He, Y.; Krishna, R.; Chen, B. Metal-Organic Frameworks with Potential for Energy-Efficient Adsorptive Separation of Light Hydrocarbons, *Energy Environ. Sci.* **2012**, *5*, 9107-9120.

(9) Dietzel, P. D. C.; Besikiotis, V.; Blom, R. Application of metal–organic frameworks with coordinatively unsaturated metal sites in storage and separation of methane and carbon dioxide, *J. Mater. Chem.* **2009**, *19*, 7362-7370.

(10) Bao, Z.; Yu, L.; Ren, Q.; Lu, X.; Deng, S. Adsorption of CO_2 and CH_4 on a magnesium-based metal organic framework, *J. Colloid Interface Sci.* **2011**, *353*, 549-556.

(11) Yaghi, O. M. Hydrogen Storage in Metal Organic Frameworks, www.hydrogen.energy.gov/pdfs/review11/st049_yaghi_2011_p.pdf, University of California Los Angeles, California, 2011.

(12) Latroche, M.; Surblé, S.; Serre, C.; Mellot-Draznieks, C.; Llewellyn, P. L.; Lee, J. H.; Chang, J. S.; Jhung, S. H.; Férey, G. Hydrogen Storage in the Giant-Pore Metal–Organic Frameworks MIL-100 and MIL-101, *Angew. Chem. Int. Ed.* **2006**, *45*, 8227-8231.

(13) Belmabkhout, Y.; Pirngruber, G.; Jolimaitre, E.; Methivier, A. A complete experimental approach for synthesis gas separation studies using static gravimetric and column breakthrough experiments, *Adsorption* **2007**, *13*, 341-349.

(14) Cavenati, S.; Grande, C. A.; Rodrigues, A. E. Adsorption Equilibrium of Methane, Carbon Dioxide, and Nitrogen on Zeolite 13X at High Pressures, *J. Chem. Eng. Data* **2004**, *49*, 1095-1101.

(15) Chen, B.; Ockwig, N. W.; Millward, A. R.; Contreras, D. S.; Yaghi, O. M., High H_2 Adsorption in a Microporous Metal-Organic Framework with Open Metal Sites. *Angew. Chem. Int. Ed.* **2005**, *44*, 4745-4749.

(16) Lin, X.; Jia, J.; Zhao, X.; Thomas, K. M.; Blake, A. J.; Walker, G. S.; Champness, N. R.; Hubberstey, P.; Schröder, M., High H_2 Adsorption by Coordination-Framework Materials. *Angew. Chem. Int. Ed.* **2006**, *45*, 7358-7364.

(17) Lee, Y.-G.; Moon, H. R.; Cheon, Y. E.; Suh, M. P., A Comparison of the H_2 Sorption Capacities of Isostructural Metal-Organic Frameworks With and Without Accessible Metal Sites: $[\{Zn_2(abtc)(dmf)_2\}_3]$ and $[\{Cu_2(abtc)(dmf)_2\}_3]$ versus $[\{Cu_2(abtc)\}_3]$. *Angew. Chem. Int. Ed.* **2008,** *47*, 7741-7745.

(18) Wang, X.-S.; Ma, S.; Rauch, K.; Simmons, J. M.; Yuan, D.; Wang, X.; Yildirim, T.; Cole, W. C.; López, J. J.; Meijere, A. d.; Zhou, H.-C., Metal-Organic Frameworks Based on Double-Bond-Coupled Di-Isophthalate Linkers with High Hydrogen and Methane Uptakes. *Chem. Mater.* **2008**, *20*, 3145-3152.

(19) Xue, M.; Zhu, G.; Li, Y.; Zhao, X.; Jin, Z.; Kang, E.; Qiu, S., Structure, Hydrogen Storage, and Luminescence Properties of Three 3D Metal-Organic Frameworks with NbO and PtS Topologies. *Cryst. Growth Des.* **2008**, *8*, 2478-2483.

(20) Sun, D.; Ma, S.; Simmons, J. M.; Li, J.-R.; Yuan, D.; Zhou, H.-C., An unusual case of symmetry-preserving isomerism. *Chem. Commun.* **2010**, *46*, 1329-1331.

(21) Zhao, D.; Yuan, D.; Yakovenko, A.; Zhou, H.-C., A NbO−type metal−organic framework derived from a polyyne-coupling di-isophthalate linker formed *in situ*. *Chem. Commun.* **2010**, *46*, 4196-4198.

(22) Ma, S.; Sun, D.; Simmons, J. M.; Collier, C. D.; Yuan, D.; Zhou, H.-C., Metal-Organic Framework from an Anthracene Derivative Containing Nanoscopic Cages Exhibiting High Methane Uptake. *J. Am. Chem. Soc.* **2008**, *130*, 1012-1016.

(23) Lin, X.; Telepeni, I.; Blake, A. J.; Dailly, A.; Brown, C. M.; Simmons, J. M.; Zoppi, M.; Walker, G. S.; Thomas, K. M.; Mays, T. J.; Hubberstey, P.; Champness, N. R.; Schröder, M., High Capacity Hydrogen Adsorption in Cu(II) Tetracarboxylate Framework Materials: The Role of Pore Size, Ligand Functionalization, and Exposed Metal Sites. *J. Am. Chem. Soc.* **2009**, *131*, 2159-2171.

(24) Yang, S.; Lin, X.; Dailly, A.; Blake, A. J.; Hubberstey, P.; Champness, N. R.; Schröder, M., Enhancement of H_2 Adsorption in Coordination Framework Materials by Use of Ligand Curvature. *Chem. Eur. J.* **2009**, *15*, 4829-4835.

(25) Prasad, T. K.; Hong, D. H.; Suh, M. P., High Gas Sorption and Metal-Ion Exchange of Microporous Metal−Organic Frameworks with Incorporated Imide Groups. *Chem. Eur. J.* **2010**, *16*, 14043-14050.

(26) Wang, X.-S.; Meng, L.; Cheng, Q.; Kim, C.; Wojtas, L.; Chrzanowski, M.; Chen, Y.-S.; Zhang, X. P.; Ma, S., Three-Dimensional Porous Metal-Metalloporphyrin Framework Consisting of Nanoscopic Polyhedral Cages. *J. Am. Chem. Soc.* **2011**, *133*, 16322-16325.

(27) Wang, X.-J.; Li, P.-Z.; Liu, L.; Zhang, Q.; Borah, P.; Wong, J. D.; Chan, X. X.; Rakesh, G.; Li, Y.; Zhao, Y., Significant gas uptake enhancement by post-exchange of zinc(II) with copper(II) within a metal-organic framework. *Chem. Commun.* **2012**, *48*, 10286-10288.

(28) Matsunaga, S.; Endo, N.; Mori, W., Microporous Porphyrin-Based Metal Carboxylate Frameworks with Various Accessible Metal Sites: [Cu_2(MDDCPP)] [M = Zn^{2+}, Ni^{2+}, Pd^{2+}, $Mn^{3+}(NO_3)$, Ru^{2+}(CO)]. *Eur. J. Inorg. Chem.* **2012**, 4885-4897.